Hydrogen storage properties and neutron scattering studies of Mg₂(dobdc)—a metal–organic framework with open Mg²⁺ adsorption sites†‡

Kenji Sumida,[ab] Craig M. Brown,[*c] Zoey R. Herm,[ab] Sachin Chavan,[d] Silvia Bordiga[d] and Jeffrey R. Long[*ab]

The hydrogen storage properties of Mg₂(dobdc) (dobdc⁴⁻ = 2,5-dioxido-1,4-benzenedicarboxylate), a metal–organic framework possessing hexagonal one-dimensional channels decorated with unsaturated Mg²⁺ coordination sites, have been examined through low- and high-pressure adsorption experiments, infrared spectroscopy, and neutron scattering studies.

Owing to their high permanent porosity, exceptional structural and chemical tunability, and convenient modular synthesis, metal–organic frameworks have recently come under intensive study for use as solid-state sorbents in gas storage applications.[1] With regard to cryogenic hydrogen storage, gravimetric and/or volumetric hydrogen storage capacities that approach the U.S. Department of Energy targets[2] for mobile systems have been demonstrated in the highest surface area materials.[1c,3] However, the performance of these materials is greatly diminished at ambient temperature due to the weak, physisorptive interactions between the internal pore surface and the hydrogen molecules. Indeed, the isosteric heat of H_2 adsorption within these materials typically lies in the range of -5 to -7 kJ mol^{-1}, which is well below the -15 kJ mol^{-1} that is considered optimal for a sorbent operating between 1.5 and 30 bar at 298 K.[4,5] The study of metal–organic frameworks with exposed metal cation sites represents one promising avenue for achieving stronger framework–H_2 interactions, and is of particular interest for light cations with a high charge density.[6,7] Herein, we report the hydrogen storage properties of Mg₂(dobdc) (MOF-74(Mg)),[7d,e] which possesses pores that are decorated with unsaturated Mg²⁺ coordination sites (see Fig. 1). Importantly, rigorous study of the adsorption properties *via* adsorption experiments, variable-temperature infrared spectroscopy, and neutron scattering methods affords a

detailed description of the loading characteristics, which is crucial for the design of next-generation materials.

The solvated form of Mg₂(dobdc) was prepared using a synthesis adapted from the literature procedure.[7d] Activation was performed by heating the material in anhydrous DMF followed by anhydrous methanol, and heating the material *in vacuo* at 180 °C. The BET surface area[8] of 1510(5) m² g^{-1} for a material activated under the optimized conditions is close to the accessible surface area[9] of 1705 m² g^{-1}, indicating the full evacuation of the pores.

The lower-pressure H_2 adsorption isotherms for an activated sample of Mg₂(dobdc) are presented in Fig. 2. Remarkably, the H_2 uptake at 77 K reaches 1 wt% at just 0.02 bar, presumably due to the high density of open metal sites within the structure. In addition, the relatively high surface area leads to the H_2

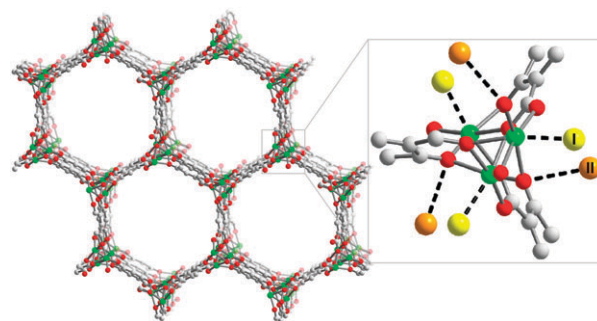**Fig. 1** A portion of the crystal structure of Mg₂(dobdc) as viewed down the [001] direction. Green, gray, and red spheres represent Mg, C, and O atoms, respectively; H atoms omitted for clarity. Inset: D₂ binding sites (site I: yellow; site II: orange) as determined by neutron diffraction.
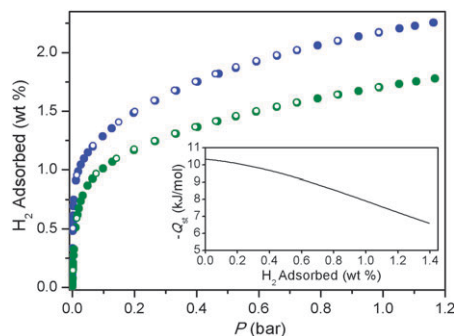

Fig. 2 Lower-pressure H_2 isotherms recorded at 77 K (blue) and 87 K (green). Filled and open symbols represent adsorption and desorption, respectively. Inset: Isosteric heat of adsorption ($-Q_{st}$) as a function of H_2 adsorbed.

a Department of Chemistry, University of California, Berkeley, California 94720, USA. E-mail: jrlong@berkeley.edu
b Materials Sciences Division, Lawrence Berkeley National Laboratory, Berkeley, CA 94720, USA
c National Institute of Standards and Technology, Center for Neutron Research, Gaithersburg, MD 20899, USA. E-mail: craig.brown@nist.gov
d Department of Chemistry, IFM & NIS Centre of Excellence, University of Torino, Via Quarello, 11 I-10135 Torino, Italy
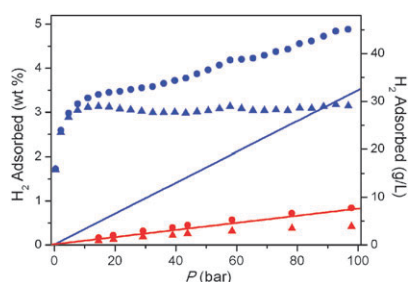
uptake (1 bar) of 2.2 wt% and 1.7 wt% at 77 K and 87 K, respectively. The zero-coverage isosteric heat of adsorption (Q_{st}) of $-10.3(2)$ kJ mol^{-1} evaluated using a virial-type fitting to the isotherm data is indicative of the polarizing nature of the exposed Mg^{2+} cations, and the gradual decrease of Q_{st} to $-7.9(2)$ kJ mol^{-1} at an adsorption level of 1 wt% is consistent with the gradual saturation of these sites.

The corresponding high-pressure H_2 adsorption isotherms recorded at 77 K and 298 K are shown in Fig. 3. At 77 K, the excess adsorption saturates at a maximum of 3.2 wt% at 15 bar, and the total adsorption reaches 4.9 wt% and 45 g L^{-1} at 100 bar. The volumetric storage capacity at 100 bar constitutes a 44% increase over the corresponding density of pure H_2 gas, and is a result of the close approach of H_2 to the framework surface facilitated by the Mg^{2+} centers. Surprisingly, despite the high density of unsaturated metal sites, the total adsorption at 298 K is just 0.8 wt% and 7.5 g L^{-1} at 100 bar, representing just a marginal improvement over the corresponding storage density of compressed H_2 gas.

The site-specific binding enthalpy at the open Mg^{2+} adsorption site was probed through variable-temperature infrared spectroscopy. Upon cooling of a sample of Mg_2(dobdc) exposed to H_2, the evolution of two absorption bands centered at 4091 and 4085 cm^{-1} is observed as shown in Fig. 4. These bands can be, respectively, assigned to *para*-H_2 (p-H_2) and *ortho*-H_2 (o-H_2) owing to their expected frequency difference (6 cm^{-1} for gas phase H_2), and by the observation of a spectral change at low temperature (*ca.* 20 K) and decreased equilibrium pressure (see Fig. S4, ESI‡). The integrated infrared absorbance was used to generate a van't Hoff-type plot (Fig. S5, ESI‡), from which the standard adsorption enthalpy ($\Delta H^0 = -12.1 \pm 1.0$ kJ mol^{-1}) and entropy ($\Delta S^0 = -137 \pm 10$ J K^{-1} mol^{-1}) could be determined. The large magnitude of ΔH^0 is consistent with the close approach of H_2 to the exposed Mg^{2+} cations. Note that this
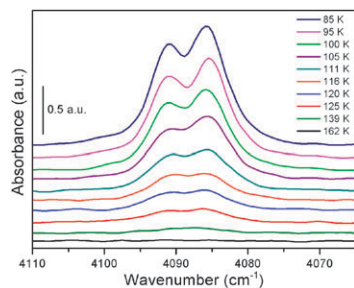
value lies slightly below the corresponding value of -13.5 kJ mol^{-1} for Ni_2(dobdc),[10] likely as a result of the slightly larger ionic radius (and lower charge density) of Mg^{2+} (0.72 Å) compared to Ni^{2+} (0.69 Å). Meanwhile, the negative sign of ΔS^0 is presumably a result of the more efficient packing and limited mobility of the adsorbed molecules compared to the bulk gas, owing to the close approach and localized adsorption of H_2.[11]

The loading-dependent H_2 adsorption characteristics were probed using powder neutron diffraction experiments performed at the BT-1 high-resolution diffractometer at the National Institute of Standards and Technology Center for Neutron Research (NCNR). At a loading of 0.6 D_2 per Mg^{2+} site, the nuclear density map indicates the highest-affinity adsorption site to be just 2.45(4) Å from the metal center (see Fig. 1). Note that this distance is in close agreement with the theoretically calculated distance of 2.50 Å evaluated using density functional theory.[12] At the same loading, a secondary binding site approximately 3.5 Å from the oxido group of the organic linker could be identified. Two further sites were located within the structure at higher loadings, although their distance from the framework surface (>4.0 Å) suggests only very weak interactions that are physisorptive in nature. These observations are also supported by the infrared spectra collected at similarly low temperatures (see Fig. S4, ESI‡).

Selected inelastic neutron scattering spectra collected at the BT-4 filter analyzer neutron spectrometer[13] (FANS) at the NCNR are shown in Fig. 5. The spectrum recorded at 4 K for the evacuated material is dominated by vibrational modes of the ligand, and bears close resemblance to the corresponding spectrum of Zn_2(dobdc) (Fig. S7, ESI‡).[14] The material was then dosed with 0.6 p-H_2 per Mg^{2+} site, resulting in three new features in the spectra at approximately 6.8, 10.4, and 24.1 meV. These new peaks are attributed to the splitting of the $J = 1$ rotational level of H_2 upon association with the open metal site. Upon increasing the loading to 1.2 p-H_2 per Mg^{2+} site, additional features between 15 and 20 meV are observed, and are attributable to H_2 adsorbed at site II.[14] The analogous data for normal-H_2 (n-H_2), which is a mixture of approximately 75% o-H_2 and 25% p-H_2, reveal three additional peaks at 14.1, 18.0, and 27.3 meV, respectively. These peaks are presumably a result of the coupling of H_2 in the $J = 1$ rotational state with the hydrogen phonons.

The corrected neutron scattering data[15] collected on the disk-chopper spectrometer[16] (DCS) at the NCNR for a loading of 1.2 n-H_2 per Mg^{2+} site are displayed in Fig. S7

Fig. 3 High-pressure H_2 isotherms recorded at 77 K (blue) and 298 K (red). Triangles and circles represent excess and total uptake, while the solid lines show the density of pure H_2 gas.
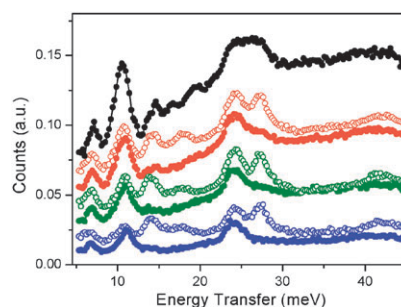

Fig. 4 Variable-temperature infrared spectra of H_2 adsorbed on activated Mg_2(dobdc) in the temperature range of 85 to 162 K.

Fig. 5 Selected INS spectra recorded at 4 K following subtraction of the spectrum of evacuated Mg_2(dobdc) for loadings of 0.2 (blue), 0.4 (green), 0.6 (orange), and 1.2 (black) H_2 molecules per Mg^{2+} site. Filled and open symbols represent data for p-H_2 and n-H_2, respectively.

(ESI‡). As reported recently,[7f] the rotational lines observed in neutron energy loss at 6.8 meV and 10.2 meV are not symmetrically observed, and only a single peak at −6.5 meV is observed with an intensity reduced by a factor of 9.[17] In the previous work, the absence of the peak at approximately −10 meV is ascribed to the presence of multiple binding sites at the Mg^{2+} site. However, we note that there is a quantum-mechanically allowed thermal population of the $J = 1$ sub-levels, wherein the lowest $J = 1$ sub-level is populated at 4 K. Such an interpretation allows the INS data to be described with just one type of H_2 adsorption site at the Mg^{2+} center, which is in agreement with the powder neutron diffraction data.

The diffusional behavior of H_2 within the one-dimensional channels of Mg_2(dobdc) was studied by quasielastic neutron scattering (QENS). Surprisingly, at a dosing of 0.33 n-H_2 per Mg^{2+} site, a QENS signal that is virtually indistinguishable from the resolution function of the instrument was obtained (Fig. S10, ESI‡). This suggests the absence of H_2 diffusion on the picosecond timescale owing to the strong interaction between H_2 and the exposed Mg^{2+} cations. However, the spectrum becomes successively broadened at higher loadings, indicative of the diffusion of H_2 associated with the weaker binding sites and bulk H_2 within the channels, respectively.

The Q-dependent spectra were fit to a hydrogen diffusion model composed of two Lorentzian functions (narrow and broad) along with an elastic contribution that was convoluted with the instrument resolution function (Fig. S11, ESI‡). The elastic response partially originates from stationary H_2, the narrow function originates from H_2 diffusing along the pore surface, and the broad function arises from bulk-like gas diffusing through the one-dimensional pores. The extracted line widths of the narrow component are indicative of a liquid-like jump-diffusion with no distinct spatial orientation of the jump direction as observed in other studies of H_2 within porous media.[18] Interestingly, the diffusion coefficients ($D = 1.2(1) \times 10^{-8}$ m^2 s^{-1} at low loading; $D = 0.51(2) \times 10^{-8}$ m^2 s^{-1} at 1 bar) derived from the fittings is an order of magnitude lower than the one-dimensional diffusion of H_2 in Cr(OH)(bdc) (bdc^{2-} = 1,4-benzenedicarboxylate; MIL-53(Cr)) and VO(bdc) (MIL-47(V)) under similar conditions,[19] and of similar magnitude to H_2 diffusing on a carbon surface.

The foregoing results describe the hydrogen storage properties of Mg_2(dobdc) as studied by adsorption experiments, infrared spectroscopy, and neutron scattering studies. The complementary nature of these techniques has afforded a complete picture of the H_2 adsorption within the material, and has revealed an alternative interpretation to the INS data recently reported, in which the data can be completely described by a single type of adsorption site at the exposed Mg^{2+} cation. We envisage that further studies of this type will afford a clearer understanding of the effect of the chemical and structural features of metal–organic frameworks on the H_2 storage properties at ambient temperatures.

Notes and references

1 (a) M. Eddaoudi, J. Kim, N. Rosi, D. Vodak, J. Wachter, M. O'Keeffe and O. M. Yaghi, *Science*, 2002, **295**, 469; (b) S. Kitagawa, R. Kitaura and S.-I. Noro, *Angew. Chem., Int. Ed.*, 2004, **43**, 2334; (c) A. R. Millward and O. M. Yaghi, *J. Am. Chem. Soc.*, 2005, **127**, 17998; (d) H. Furukawa, M. A. Miller and O. M. Yaghi, *J. Mater. Chem.*, 2007, **17**, 3197; (e) G. Férey, *Chem. Soc. Rev.*, 2008, **37**, 191; (f) S. Ma, D. Sun, J. M. Simmons, C. D. Collier, D. Yuan and H.-C. Zhou, *J. Am. Chem. Soc.*, 2008, **130**, 1012; (g) R. E. Morris and P. S. Wheatley, *Angew. Chem., Int. Ed.*, 2008, **47**, 4966; (h) L. J. Murray, M. Dincă and J. R. Long, *Chem. Soc. Rev.*, 2009, **38**, 1294.
2 EERE: Hydrogen, Fuel Cells, & Infrastructure Technologies Program http://www.eere.energy.gov/hydrogenandfuelcells, accessed August 2010.
3 (a) M. Latroche, S. Surblé, C. Serre, C. Mellot-Draznieks, P. L. Llewellyn, J.-H. Lee, J.-S. Chang, S. H. Jhung and G. Férey, *Angew. Chem., Int. Ed.*, 2006, **45**, 8227; (b) S. S. Kaye, A. Dailly, O. M. Yaghi and J. R. Long, *J. Am. Chem. Soc.*, 2007, **129**, 14176; (c) K. Sumida, M. R. Hill, S. Horike, A. Dailly and J. R. Long, *J. Am. Chem. Soc.*, 2009, **131**, 15120; (d) K. Koh, A. G. Wong-Foy and A. J. Matzger, *J. Am. Chem. Soc.*, 2009, **131**, 4184.
4 S. K. Bhatia and A. L. Myers, *Langmuir*, 2006, **22**, 1688.
5 Note that the consideration of an enthalpy–entropy correlation for H_2 adsorption in metal–organic frameworks results in an even greater magnitude for the optimal enthalpy of adsorption (−20 to −25 kJ mol^{-1}): (a) E. Garrone, B. Bonelli and C. Otero Areán, *Chem. Phys. Lett.*, 2008, **456**, 68; (b) C. Otero Areán, S. Chavan, C. P. Cabello, E. Garrone and G. T. Palomino, *ChemPhysChem*, 2010, **11**, 3237.
6 (a) M. Dincă and J. R. Long, *J. Am. Chem. Soc.*, 2005, **127**, 9376; (b) A. Vimont, J.-M. Goupil, J.-C. Lavalley, M. Daturi, S. Surblé, C. Serre, F. Millange, G. Férey and N. Audebrand, *J. Am. Chem. Soc.*, 2006, **128**, 3218; (c) H. R. Moon, N. Kobayashi and M. P. Suh, *Inorg. Chem.*, 2006, **45**, 8672; (d) M. Dincă, A. Dailly, Y. Liu, C. M. Brown, D. A. Neumann and J. R. Long, *J. Am. Chem. Soc.*, 2006, **128**, 16876; (e) K. Sumida, S. Horike, S. S. Kaye, Z. R. Herm, W. L. Queen, C. M. Brown, F. Grandjean, G. J. Long, A. Dailly and J. R. Long, *Chem. Sci.*, 2010, **1**, 184.
7 (a) P. D. C. Dietzel, Y. Morita, R. Blom and H. Fjellvag, *Angew. Chem., Int. Ed.*, 2005, **44**, 6354; (b) N. L. Rosi, J. Kim, M. Eddaoudi, B. Chen, M. O'Keeffe and O. M. Yaghi, *J. Am. Chem. Soc.*, 2005, **127**, 1504; (c) P. D. C. Dietzel, B. Panella, M. Hirscher, R. Blom and H. Fjellvag, *Chem. Commun.*, 2006, 959; (d) S. R. Caskey, A. G. Wong-Foy and A. J. Matzger, *J. Am. Chem. Soc.*, 2008, **130**, 10870; (e) P. D. C. Dietzel, R. Blom and H. Fjellvag, *Eur. J. Inorg. Chem.*, 2008, 3624; (f) P. D. C. Dietzel, P. A. Georgiev, J. Eckert, R. Blom, T. Strässle and T. Unruh, *Chem. Commun.*, 2010, **46**, 4962.
8 K. S. Walton and R. Q. Snurr, *J. Am. Chem. Soc.*, 2007, **129**, 8552.
9 T. Düren, F. Millange, G. Férey, K. S. Walton and R. Q. Snurr, *J. Phys. Chem. C*, 2007, **111**, 15350.
10 J. G. Vitillo, L. Regli, S. Chavan, G. Ricchiardi, G. Spoto, P. D. C. Dietzel, S. Bordiga and A. Zecchina, *J. Am. Chem. Soc.*, 2008, **130**, 8386.
11 Y. Liu, H. Kabbour, C. M. Brown, D. A. Neumann and C. C. Ahn, *Langmuir*, 2008, **24**, 4772.
12 W. Zhou, H. Wu and T. Yildirim, *J. Am. Chem. Soc.*, 2008, **130**, 15268.
13 T. J. Udovic, C. M. Brown, J. B. Leao, P. C. Brand, R. D. Jiggetts, R. Zeitoun, T. A. Pierce, I. Peral, J. R. D. Copley, Q. Huang, D. A. Neumann and R. J. Fields, *Nucl. Instrum. Methods Phys. Res., Sect. A*, 2008, **588**, 406.
14 L. Kong, G. Román-Pérez, J. M. Soler and D. C. Langreth, *Phys. Rev. Lett.*, 2009, **103**, 096103.
15 R. T. Azuah, L. R. Kneller, Y. Qiu, P. L. W. Tregenna-Piggott, C. M. Brown, J. R. D. Copley and R. M. Dimeo, *J. Res. Natl. Inst. Stand. Technol.*, 2009, **114**, 241.
16 J. R. D. Copley and J. C. Cook, *Chem. Phys.*, 2003, **292**, 477.
17 J. A. Young and J. U. Koppel, *Phys. Rev. A*, 1964, **135**, 603.
18 (a) M. Bienfait, P. Zeppenfeld, R. C. Ramos, J. M. Gay, O. E. Vilches and G. Coddens, *Phys. Rev. B*, 1999, **60**, 11773; (b) D. G. Narehood, J. V. Pearce, P. C. Eklund, P. E. Sokol, R. E. Lechner, J. Pieper, J. R. D. Copley and J. C. Cook, *Phys. Rev. B*, 2003, **67**, 5; (c) O. E. Haas, J. M. Simon, S. Kjelstrup, A. L. Ramstad and P. Fouquet, *J. Phys. Chem. C*, 2008, **112**, 3121.
19 F. Salles, D. I. Kolokolov, H. Jobic, G. Maurin, P. L. Llewellyn, T. Devic, C. Serre and G. Férey, *J. Phys. Chem. C*, 2009, **113**, 7802.